IEEE Access
Multidisciplinary | Rapid Review | Open Access Journal

Received December 23, 2018, accepted February 6, 2019, date of publication February 25, 2019, date of current version March 7, 2019.

Digital Object Identifier 10.1109/ACCESS.2019.2900280

A Formation Collision Avoidance System for Unmanned Surface Vehicles With Leader-Follower Structure

XIAOJIE SUN, GUOFENG WANG, YUNSHENG FAN, DONGDONG MU, AND BINGBING QIU
College of Marine Electrical Engineering, Dalian Maritime University, Dalian 116026, China

Corresponding author: Guofeng Wang (gfwangsh@163.com)

This work was supported in part by the Nature Science Foundation of China under Grant 51609033, in part by the Nature Science Foundation of Liaoning Province of China under Grant 20180520005, and in part by the Fundamental Research Funds for the Central Universities under Grant 3132018306 and Grant 3132016312.

ABSTRACT This paper deals with the problem of formation collision avoidance for unmanned surface vehicles (USVs). Compared with the generalship formation, the formation collision avoidance system (FCAS) needs better responsiveness and stability because of faster speed and smaller volume for USVs. A method based on finite control set model predictive control is proposed to solve this problem. The novelty of the method is that it can control formation quickly to avoid obstacles and reach the destination in accordance with the dynamics of each vessel in the formation, without the prior knowledge of the environment and reference trajectory. The thruster speed and propulsion angle of the USV form a finite control set, which is more practical. The FCAS adopts the leader–follower structure and distributed control strategy to ensure that the followers have a certain autonomy. The first two simulation tests verify that the system has the formation stability, formation forming ability, and the applicability in restricted water. The last simulation test shows that the system can control the USV formation to sail quickly and safely in complex sea scenarios with formation transformation task and multiple dynamic obstacles.

INDEX TERMS Unmanned surface vehicles, formation collision avoidance system, finite control set, model predictive control, leader-follower structure.

I. INTRODUCTION

As unmanned surface vehicles (USVs) are finding increased utility in both military and commercial applications, their research are gaining importance [1]. In the process of achieving a mission, more than one USV is often needed, so the coordination of USV formation needs to be considered. The USV formation can improve the robustness and fault-tolerant resilience of the USV, improve mission performance, reduce the operating cost, and extend the coverage of application strategies such as monitoring, communication and measurement [2]. So much of the focus of recent USV research has shifted to USV formation issues.

In terms of USV formation, the main control goal at present is to design a series of controllers for each vessel in the formation to ensure tracking and maintaining the desired positions and orientations. In the presence of modeling uncertainties and time-varying external disturbances, scholars have adopted many advanced control algorithms for USV formation, including neural network control [3], [4], disturbance observers [3], [4], dynamic surface control technique [3], sliding mode control [5], input-output linearization technique [6], adaptive feedback control [7], back-stepping control [8]. And Chen et al. consider the problem of guiding the underactuated ship formation to track a general kind of non-convex, closed curves, and eventually achieve attitude synchronization [8]. Next, considering the convergence time of the controller, finite time formation control is also very important. In [9], based on terminal sliding-mode observer, a novel disturbance estimation scheme is proposed to achieve high-accuracy formation control of multiple vessels, which can accurately estimate external disturbance after finite time. Literature [10] presented a fault tolerant leader-follower formation control scheme for underactuated USV formation, and although there are actuator faults and system uncertainties, the formation tracking errors can converge into arbitrarily small neighborhoods around zero in finite time. Gao and Guo [11] investigate a fixed-time leader-follower

The associate editor coordinating the review of this manuscript and approving it for publication was Zhixiong Peter Li.

formation control method for autonomous underwater vehicles (AUVs) with event-triggered acoustic communications. Aiming at the communication problem (network-induced delays and packet dropouts) of USV formation, an incremental predictive control scheme is adopted to ensure that outputs of all USVs in the formation reach consensus asymptotically in [12]. In the formation control strategies, the most common control strategy for USVs is the leader-follower control [5], [10]–[12], and for other unmanned platforms, there are the behavior-based formation control [13], [14] and the virtual structure approach [13], [15]. However, most of the literatures only consider the internal control problem in the USV formation, and do not consider the formation control problem in complex environmental constraints.

In the system structure of guidance, navigation, and control (GNC), formation path planning is used to solve this problem. The formation path planning algorithm generates the collision-free optimal path or way-points for each individual of the formation in clutter environment, and the controller is responsible for tracking the generated trajectory. Based on GNC system structure, Hao and Agrawal [16] first proposed a planning and control framework for unmanned ground vehicle formation by using the A* algorithm. Saska *et al.* [17] then employ this framework and replace the A* by the Particle Swarm Optimization (PSO) and spline-path planning to generate better trajectories. In the same way, Liu and Bucknall [18] replace the A* by the fast marching method (FMM) for USV formation path planning in a practical maritime environment. Urcola *et al.* [19] further refine the formation path planning into local path planning and global path planning, and obtained optimal formation path through traversability maps.

However, both the path planner and controller need a lot of computing resources, which hardly meet the real-time requirement of USV formation [20]. And because the planner and the controller are separated, the planner rarely considers the motion characteristics of the vessel, which may make it difficult for the controller to track the planned path.

In order to combine path planner and controller, the idea from optimization-based control can be adopted. In vehicles formation problem, model predictive control (MPC) is increasingly applied [21]–[23]. However, due to the heavy computational load of MPC method, its application in formation control is restricted [23]. Therefore, we use the finite control set model predictive control (FCS-MPC) to reduce the computational load of MPC while preserving the advantages of MPC, such as inherent decoupling, multi-objective optimization, and nonlinear constrained optimization [24].

The literature [18] mentions the formation forming requirement, which is particularly important for formation navigation of USVs. Most of the literature on formation problem has assumed that formation has been formed before starting control. However, this situation is very unreasonable. In practice, although the desired formation shape can be formed at the beginning, the formation shape needs to be changed according to the requirements in the process of task execution, so the formation forming problem needs to be considered.

Finally, the main contributions of the proposed approach are:

1) The FCAS for USV formation is designed in accordance with the theory of FCS-MPC, which not only combines path planner with controller, but also reduces computational load.
2) Instead of force and torque, the thruster speed and propulsion angle are the control outputs of the FCAS, which is more practical.
3) The FCAS can cluster multiple USVs and ensure that each individual has a certain autonomy through the leader-follower structure and distributed control strategy.
4) Under the premise of fully considering the dynamic characteristics of underactuated USV, the FCAS can control the USV formation in the complex simulation environments, and has the formation stability, formation forming ability and the applicability in restricted water.

The rest of the paper is organized as follows. Section II briefly introduces the USV system structure. Section III gives the collision avoidance system (CAS) based on FCS-MPC method for single USV with its mathematical model. On the basis of the CAS, Section IV puts forward the FCAS for USV formation by using the leader-follower structure and distributed control strategy. Section V is the simulation result verification. Finally, Section VI concludes this paper and discusses the future works.

II. THE OVERVIEW OF USV SYSTEM

Before discussing the FCAS, a single USV system structure needs to be introduced. This study is based on Lanxin USV of Dalian Maritime University, which is a podded propulsion USV. The hierarchical structure of Lanxin USV system is illustrated in Figure 1. It is divided into four layers, including Perception layer, Task layer, Decision layer and

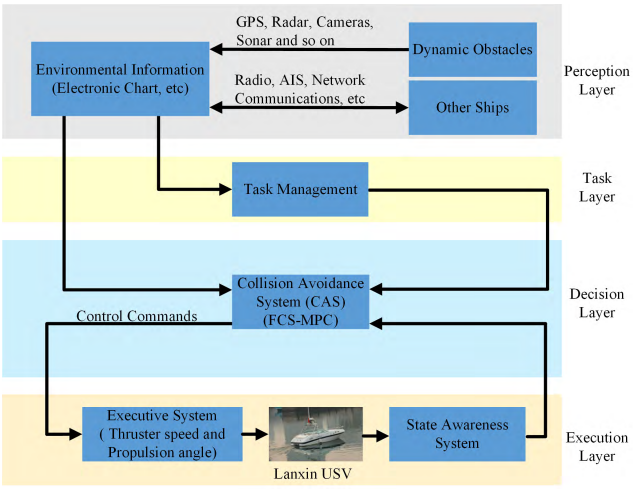

FIGURE 1. The hierarchical structure of USV system.

Execution layer. And the Decision layer connects the other three layers. The CAS based on FCS-MPC is the main component of the Decision layer. The Perception layer is responsible for perceiving the information of the surrounding environment, and the Task layer assigns the target point according to the mission. Their information is transmitted to the Decision layer, and the control commands are generated from the Decision layer to the Execution layer.

In the FCAS for USVs, a distributed control architecture is adopted, that is, each individual must carry such a CAS, so that each has certain autonomy. The detailed description of CAS and FCAS are given in Section III and IV.

III. COLLISION AVOIDANCE SYSTEM FOR USV

A. MATHEMATICAL MODEL OF USV PLANE MOTION

Assuming the ocean environment is calm, the external disturbances are neglected; the USV has x-y plane of symmetry, and its geometric center coincides with the barycenter. The mathematical model of the USV moving in surge, sway and yaw is derived using the Lagrangian mechanics [25] by neglecting motion in heave, pitch and roll can be describes as

$$\begin{cases} \dot{x} = u\cos\psi - v\sin\psi \\ \dot{y} = u\sin\psi + v\cos\psi \\ \dot{\psi} = r \\ \dot{u} = \dfrac{m_{22}}{m_{11}}vr - \dfrac{d_{11}}{m_{11}}u + \dfrac{1}{m_{11}}\tau_u \\ \dot{v} = -\dfrac{m_{11}}{m_{22}}ur - \dfrac{d_{22}}{m_{22}}v + \dfrac{1}{m_{22}}\tau_v \\ \dot{r} = \dfrac{m_{11}-m_{22}}{m_{33}}uv - \dfrac{d_{33}}{m_{33}}r + \dfrac{1}{m_{33}}\tau_r, \end{cases} \tag{1}$$

where (x, y) denotes the surge, sway displacement of the center of mass, ψ is the course angle of the vessel in the earth-fixed frame, (u, v, r) are the surge, sway and yaw velocities respectively expressed in the body-fixed frame. The terms m_{ii} denote the vessel inertia and added mass, while d_{ii} represent the hydrodynamic damping. (τ_u, τ_v, τ_r) are the surge thrust, sway thrust and yaw moment.

Additionally the propulsion force of podded propulsion USV can be regarded as a vector force T, which in different directions is [26], [27]

$$\begin{cases} \tau_u = T\cos(\delta_r) \\ \tau_v = T\sin(\delta_r) \\ \tau_r = T\sin(\delta_r)L/2, \\ T = \left(1 - t_p\right)\rho n^2 D_p^4 K_T \end{cases} \tag{2}$$

where δ_r is the propulsion angle of the steering gear output, L is the USV length.

The steering gear response model is a second-order system [28], [29], which is

$$\ddot{\delta}_r + 2\zeta\omega_n\dot{\delta}_r + \omega_n^2\delta_r = K\omega_n^2\delta \tag{3}$$

with $|\delta_r| \leq 30°$.

The state quantity X of USV includes the outputs and inputs of its model, as

$$X = [x, y, \psi, u, v, r, \delta, n]^T. \tag{4}$$

B. THE CONTROL STRATEGY

The MPC approach uses the controlled system model to predict its future behavior subject to series of control actions, and then selects the best next control action according to an objective-based cost function. When the control actions comes from a series of discrete candidate control actions (finite control set S), this method is called FCS-MPC.

For the CAS of USV based on FCS-MPC, the proposed schematic can be described as Figure 2. At the t_k instant, the control sequence $S_i(t_k)$ is generated according to the state quantity $X(t_k)$ of the current time. The future state $X_{pi}(t_{k+p})$ for each control set $S_i(t_k)$ can be predicted by the USV model $f_p(X, S)$, and t_p is the prediction time. The $X_{pi}(t_{k+p})$ is evaluated by a user-defined cost function $J(X_{pi}, S_i)$ with the constraint of target point, environment model.

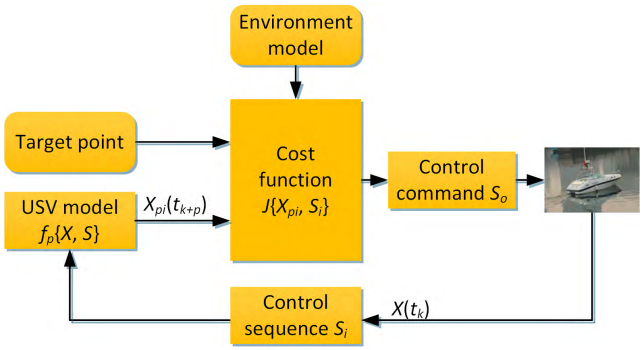

FIGURE 2. The control strategy block diagram.

C. FINITE CONTROL SET FOR USV

For the USV, the two control actions δ and n are discretized with their discrete quantities δ_d and n_d in discrete time interval Δt. However, due to the constraints of USV actuators, the δ and n are constrained by change rate $\dot{\delta}, \dot{n}$ and the actuator range. The change rate constraint is

$$S = \left\{ (\delta, n) \,\middle|\, \begin{matrix} \delta \in [\delta - \dot{\delta}\Delta t, \delta + \dot{\delta}\Delta t] \\ n \in [n - \dot{n}\Delta t, n + \dot{n}\Delta t] \end{matrix} \right\}. \tag{5}$$

The actuator range is

$$S_m = \{\delta \in [-\delta_m, \delta_m], n \in [0, n_m]\}. \tag{6}$$

And the amounts of control sets is

$$c = (2\dot{\delta}\Delta t/\delta_d) \times (2\dot{n}\Delta t/n_d). \tag{7}$$

If the values of δ_d and n_d are small, the controller will be more accurate, but the amount of computation will increase. So it is necessary to choose appropriate δ_d and n_d.

D. THE COST FUNCTION

The control sequence S_i with the greatest cost function $J(X_{pi}, S_i)$ is optimal. The cost function consists of four sub-functions, which correspond to four demands of attainability, safety, stability and rapidity [30], as

$$\begin{cases} f_1(X_{pi}, S_i) = \pi - \theta_{pi} \\ f_2(X_{pi}, S_i) = do_i \\ f_3(X_{pi}, S_i) = \delta_m - |\delta_i| \\ f_4(X_{pi}, S_i) = V_{pi}. \end{cases} \tag{8}$$

The attainability subfunction $f_1(X_{pi}, S_i)$ is related to the angle θ_{pi} between the predicted course ψ_{pi} and navigation angle, as shown in Figure 3. The safety subfunction $f_2(X_{pi}, S_i)$ can be described by the minimum distance do_i between vessel and z obstacles Xo in a distance range d_r. The propulsion angle δ and speed V of USV can depict the stability and rapidity.

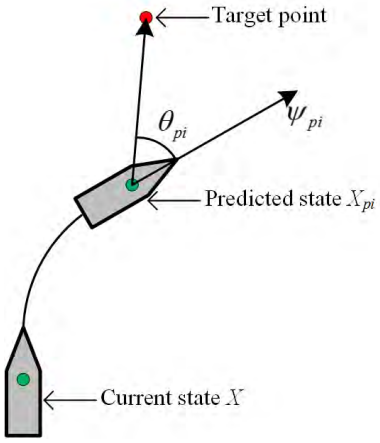

FIGURE 3. Description attainability subfunctions.

And

$$do_i = \begin{cases} \min\limits_{k=1}^{z} \{\bar{X}o_k\} & \text{if } \bar{X}o_k \le d_r \\ d_{\max} & \text{else.} \end{cases}$$
$$\bar{X}o_k = |Xo_k - X_{pi}|$$

where the Xo_k is the state quantity of the kth obstacle.

Moreover, the stop distance d_{stop} of USV is calculated by

$$d^i_{stop} = {V_{pi}}^2/(2 \cdot \dot{V}_{pi}). \tag{9}$$

When $d^i_{stop} > do_i$, the ith control action S_i is removed.

Then these subfunctions are smoothed by the normalization method, for example, the normalized attainability subfunction is

$$\bar{f}_1(X_{pi}, S_i) = \frac{f_1(X_{pi}, S_i)}{\sum_{i=1}^{c} f_1(X_{pi}, S_i)}. \tag{10}$$

The cost function with four weighting factors (w_1, w_2, w_3, w_4) is

$$J(X_{pi}, S_i) = w_1 \cdot \bar{f}_1(X_{pi}, S_i) + w_2 \cdot \bar{f}_2(X_{pi}, S_i) + w_3 \cdot \bar{f}_3(X_{pi}, S_i) + w_4 \cdot \bar{f}_4(X_{pi}, S_i). \tag{11}$$

Finally, the optimal control command S_o is selected through cost function to ensure the USV to complete the task safely and quickly.

IV. FORMATION COLLISION AVOIDANCE SYSTEM

A. THE SYSTEM STRUCTURE

For the formation collision avoidance problem of USVs, a formation collision avoidance system (FCAS) based on the single CAS is proposed with the system structure shown in Figure 4. The system adopts leader-follower approach to form formation shape, which selects one USV from the formation as the Leader and guides other USVs (Followers) to maintain formation navigation by the method of generating the sub-target [18]. According to the distributed control strategy, the CAS is applied to each USV to follow its target point individually.

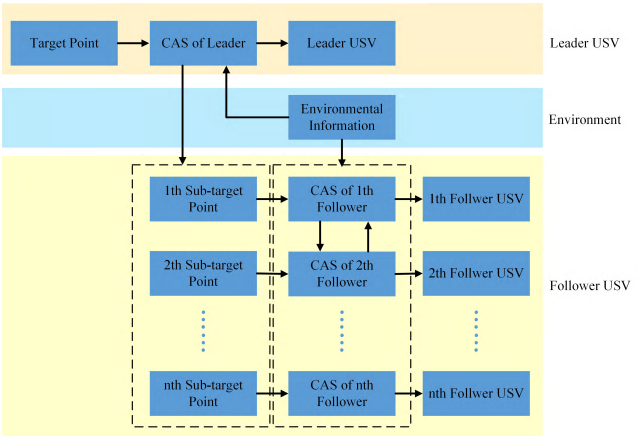

FIGURE 4. The structure of FCAS for USVs.

B. SUB-TARGET GENERATION

The principle of sub-target generation is based on the leader-follower scheme, which can flexibly generate sub-targets to make the formation deformable according to the surrounding environment. The sub-target is calculated from the desired formation shape parameters according to the position of the Leader. In Figure 5, the desired formation shape parameters are the formation angle (β) and formation distance (d) [18].

The β determines the bearing of the Follower around the Leader, and the d represents the relative distance between the Leader and the Follower. The desired formation configuration vector $\vec{D}$ can be expressed by β and d, as

$$\vec{D} = d\cos(\beta)\vec{i} + dsin(\beta)\vec{j}, \tag{12}$$

where $\vec{i}$ is the unit vector in the opposite direction to the course of Leader and $\vec{j}$ is the unit vector perpendicular to the course.

According to the Leader's position P_L, the desired position of the Follower can be calculated as

$$P_d = P_L - \vec{D}. \tag{13}$$

In the collision avoidance algorithm, when the USV approaches the target point, the algorithm will reduce the

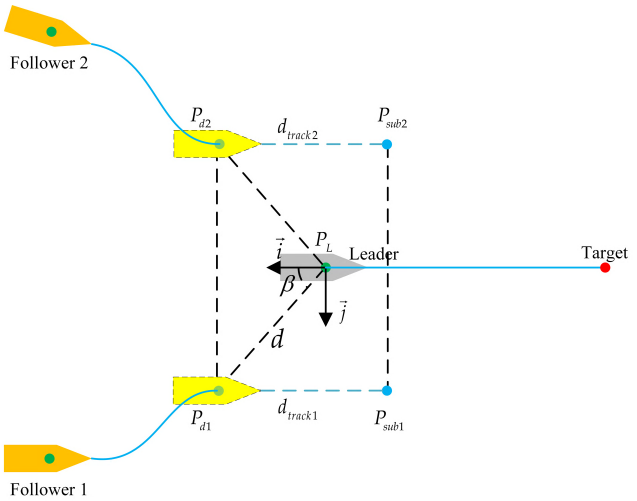

FIGURE 5. Sub-target points generation illustration.

speed of the USV and make the USV reach the target smoothly. So it is necessary to maintain a certain tracking distance $d_{track} = V_L t_p$ between the tracking sub-target and its Follower. On the other hand, in order to make tracking more accurate, the proportional-differential (PD) regulator is introduced to adjust the position of the sub-target according to the error e_i, e_j in $\vec{i}$ and $\vec{j}$ directions, and the adjustment variables are expressed as

$$\begin{cases} r_i = k_p e_i(k) + k_d \left[e_i(k) - e_i(k-1)\right] \\ r_j = k_p e_j(k) + k_d \left[e_j(k) - e_j(k-1)\right], \end{cases} \tag{14}$$

where k_p, k_d are the proportional and differential coefficients of the regulator.

So the configuration vector of the sub-target is

$$\vec{D}_s = d_{si}\vec{i} + d_{sj}\vec{j}, \tag{15}$$

among

$$\begin{cases} d_{si} = d\cos(\beta) - d_{track} + r_i \\ d_{sj} = d sin(\beta) + r_j. \end{cases}$$

And the position of the sub-target is

$$P_{sub} = P_L - \vec{D}_s. \tag{16}$$

However, by following Equations (15) and (16), the formation shape cannot be flexible. Such formation is not practical for USV navigating in restricted waters. To solve this problem, formation needs to be adjusted according to the hazard of surrounding environment. For hazard assessment, the minimum distance between obstacles and USVs can be used as an evaluation index. And the hazard is $\Xi = do/d_r$, which is the range from 0 to 1.With the increase of its value, the hazard of vessel is lower. When the hazard is higher, the change that the formation needs to do is bigger, so the hazard can be used as the deformation parameter $B = \Xi$. And in order to avoid sub-target entering obstacles, the minimum hazard of the sub-target and the corresponding kth USV should be calculated as the deformation parameter B_k.

So, the sub-targets generation equations for k Followers are updated to

$$\begin{aligned} \vec{D}_{s1} &= d_{si1}\vec{i} + B_1 d_{sj1}\vec{j}, \cdots, \\ \vec{D}_{sk} &= (\frac{k - B_k}{k-1}) d_{sik}\vec{i} + B_k d_{sjk}\vec{j}, \quad k \geq 2 \& k \in N. \end{aligned} \tag{17}$$

Here, when the deformation parameter (B_1 or B_k) values is closer to 0, the distance value in the direction of $\vec{j}$ decreases and the $\vec{i}$ direction increases, that is to say, with the decrease of the security, the formation's shape is contracted to a straight line. The parameter k represents the priority of each Follower. With the increase of the k value, the sub-target of the Follower needs to make more adjustments. When $k = 2$, the maximum distance difference in $\vec{i}$ direction is $2d_{si2} - d_{si1}$. However, such distance difference may be equal to 0, thus setting a

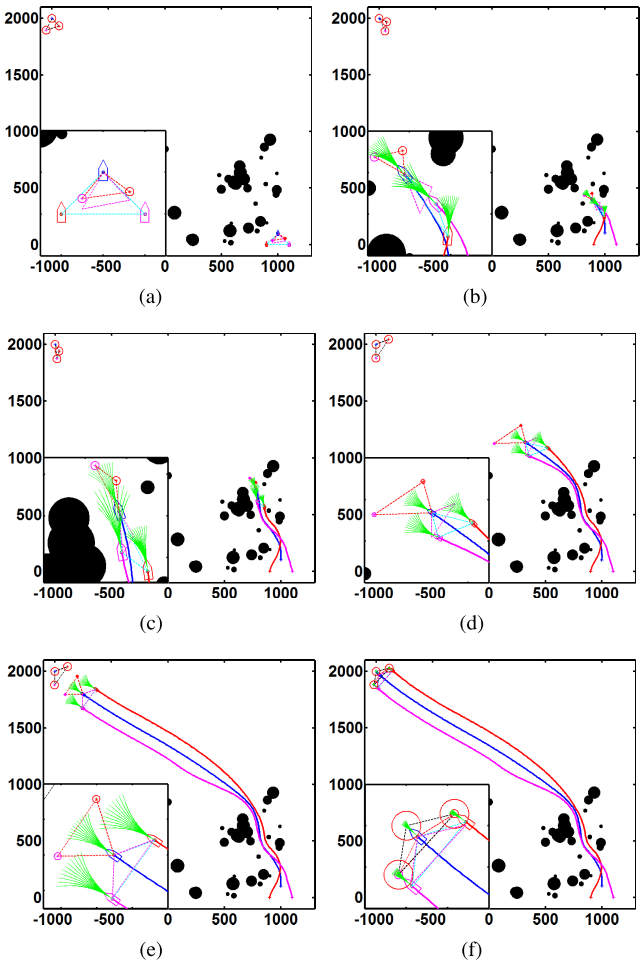

FIGURE 6. The motion sequence diagram of Test one. (a) Time 1 s. (b) Time 42 s. (c) Time 80 s. (d) Time 139 s. (e) Time 250 s. (f) Time 281 s.

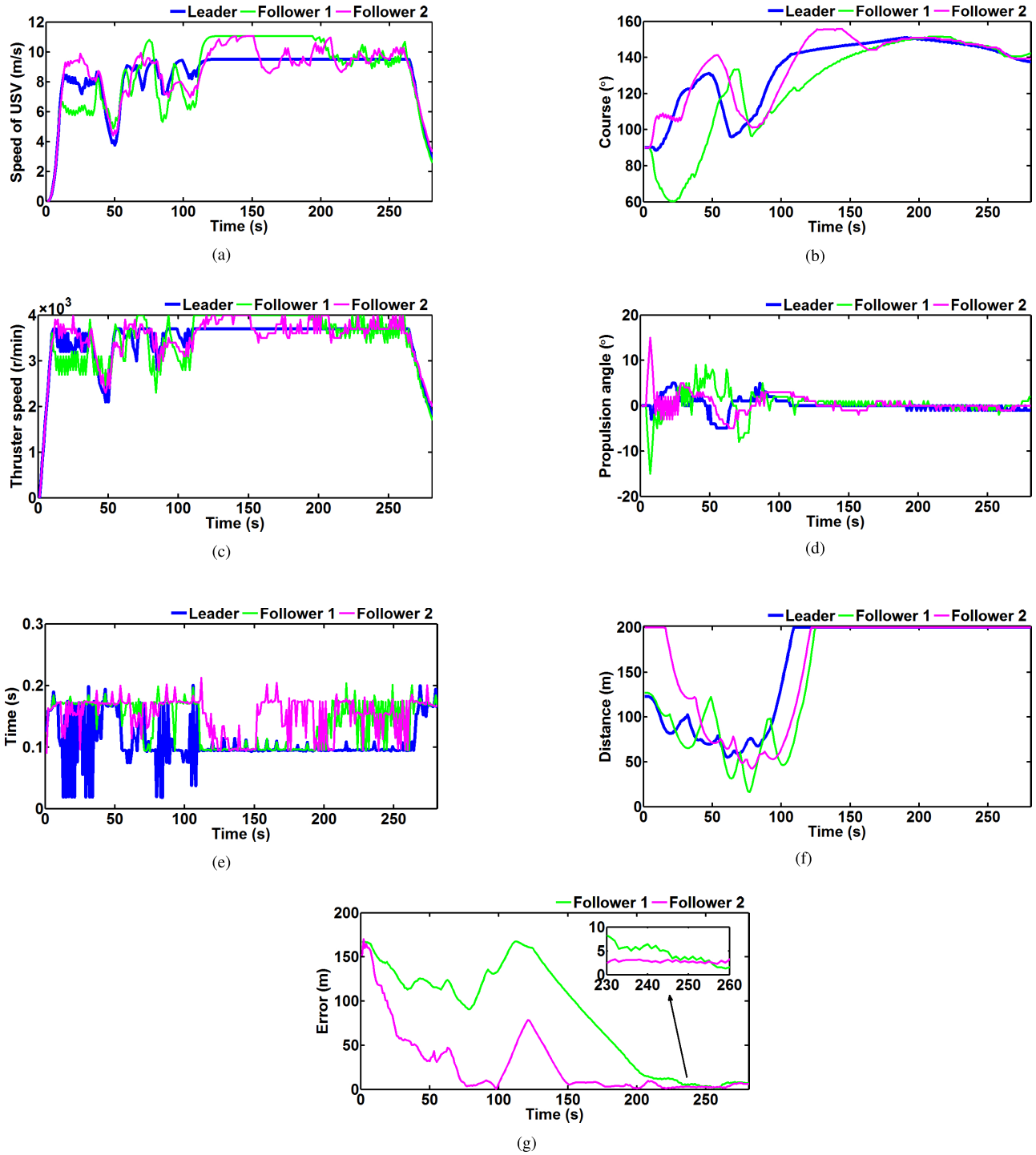

FIGURE 7. Evaluation results of Test one. (a) Speed V of USV. (b) Course ψ of USV. (c) Thruster speed n. (d) Propulsion angle δ. (e) Computation time T. (f) Distance D between obstacles and USV. (g) Formation keeping error E.

fixed distance difference d_i to adjust positions, that is

$$\vec{D}_{sk} = \left[\frac{k - B_k}{k - 1} d_{sik} + (1 - B_k) d_i\right] \vec{i} + B_k d_{sjk} \vec{j}. \quad (18)$$

In addition, due to the existence of hazard, error adjustment is meaningless, so when $B > b, b \in [0, 1)$, the regulator's coefficient is $k_p = k_d = 0$.

C. FOLLOWER'S COLLISION AVOIDANCE SYSTEM

The significant difference between the single vessel and the formation collision avoidance is to increase the problem of internal collision avoidance within the formation. Because of the distributed control structure, other USVs can be regarded as the additional obstacles called the ''internal obstacle'' in the CAS of each Follower. The CAS of the Follower is basi-

TABLE 1. Parameter information of the USVs and FCAS.

	Parameter	Value	Units
USVs	ψ_0	90.0	°
	V_0	0.0 (0.0)	m/s (kn)
	n_0	0.0	r/min
	n_m	66.7 (4000)	r/s (r/min)
	$\dot{n}$	6.7	r/s^2
	n_d	1.7 (100)	r/s (r/min)
	δ_0	0.0	°
	δ_m	30.0	°
	$\dot{\delta}$	5.0	°/s
	δ_d	1.0	°
FCAS	d_a	500.0	m
	d_r	200.0	m
	t_p	15.0	s
	Δt_c	1.0	s
	n_c	8.3 (500)	r/s (r/min)
	w_1, w_2, w_3, w_4	1.0, 2.0, 1.0, 0.5	–

TABLE 2. Results of evaluation index about USVs in test one.

USV	Index	V(m/s)	n(r/min)	δ(°)	T(s)	D(m)
Leader	maximum	9.5	3700	5.0	0.20	200.0
	minimum	0.0	0	-5.0	0.02	54.9
	average	8.4	3450	0.1	0.11	157.7
Follower 1	maximum	11.1	4000	9.0	0.20	200.0
	minimum	0.0	0	-15.0	0.09	16.4
	average	8.7	3475	0.4	0.14	147.9
Follower 2	maximum	11.1	4000	15.0	0.21	200.0
	minimum	0.0	0	-5.0	0.09	42.8
	average	8.7	3493	0.4	0.15	159.5

cally same as that of the Leader except that its tracking target and safety subfunction $f_2(X_{pi}, S_i)$. In the safety subfunction of Follower, the obstacles include internal obstacle (Leader and other Followers), and the position of internal obstacles are the predicted positions from their CAS.

In order to better maintain formation, the Leader's maximum thruster speed n_{Lm} should be slightly lower than the Followers to ensure that the Followers have the ability to follow the Leader. The above goal can be achieved by limiting the maximum thruster speed $\bar{n}_{Lm}$ of the Leader, as

$$n_{F0} = \min(n_{F1}, n_{F2}, \cdots, n_{Fk}) \tag{19}$$

$$\bar{n}_{Lm} = \min(n_{F0} + n_c, n_{Lm}), \tag{20}$$

where n_{Fk} is the thruster speed of kth Follower, n_c is the adjustment range of the thruster speed.

The formation transformation task of Followers can be accomplished only by changing their sub-targets. The sudden change from current P_{sub} to desired P^*_{sub} sub-target will cause instability of the system, so a transition sub-target $\tilde{P}_{sub}$ is needed from time t_1 to t_2, as

$$\tilde{P}_{sub} = P_{sub} + (P^*_{sub} - P_{sub})\frac{t - t_1}{t_2 - t_1}, \quad t \in [t_1, t_2]. \tag{21}$$

Through the above methods, we can achieve a USV clusters including multiple Followers.

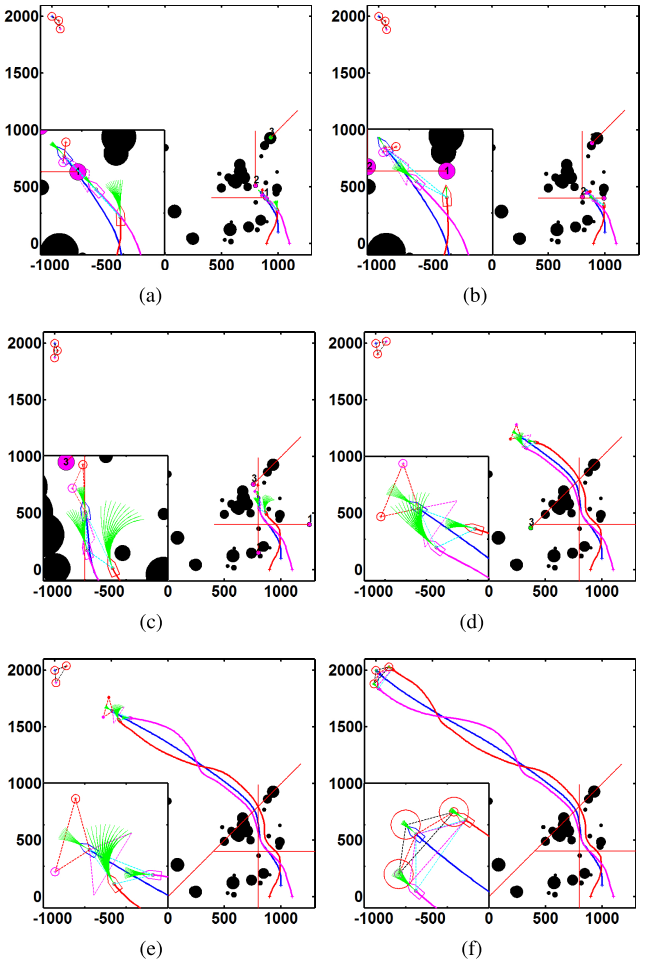

FIGURE 8. The motion sequence diagram of Test two. (a) Time 49 s. (b) Time 59 s. (c) Time 85 s. (d) Time 162 s. (e) Time 247 s. (f) Time 308 s.

V. SIMULATION STUDIES

To demonstrate the performance of the proposed FCAS for USV formation, we perform simulation in three different testing environments. The formation includes a Leader and two Followers, and the desired formation shape is an isosceles triangle with its parameters d and β are 120 m and 55°. The first test includes three scenarios: formation disorder, restricted water, and open water. They respectively test the formation forming ability, the applicability in restricted water, and the formation stability. On the basis of the first test environment, second test adds dynamic obstacles and formation transformation tasks to further test the first two performances. Finally, to verify the ability to solve the real situation for system, the third test runs in an actual sea scene with formation transformation task and multiple dynamic obstacles.

The parameters of the USVs and FCAS are in Table 1. The ψ_0, V_0, n_0 and δ_0 are the initial course, USV speed, thruster speed and propulsion angle. And to maintain the formation shape, the maximum speed n_{Lm} of the Leader is limited to 61.7 r/s (3700 r/min). Δt_c is the control update interval. The dynamic obstacles are obtained in the detection area d_a.

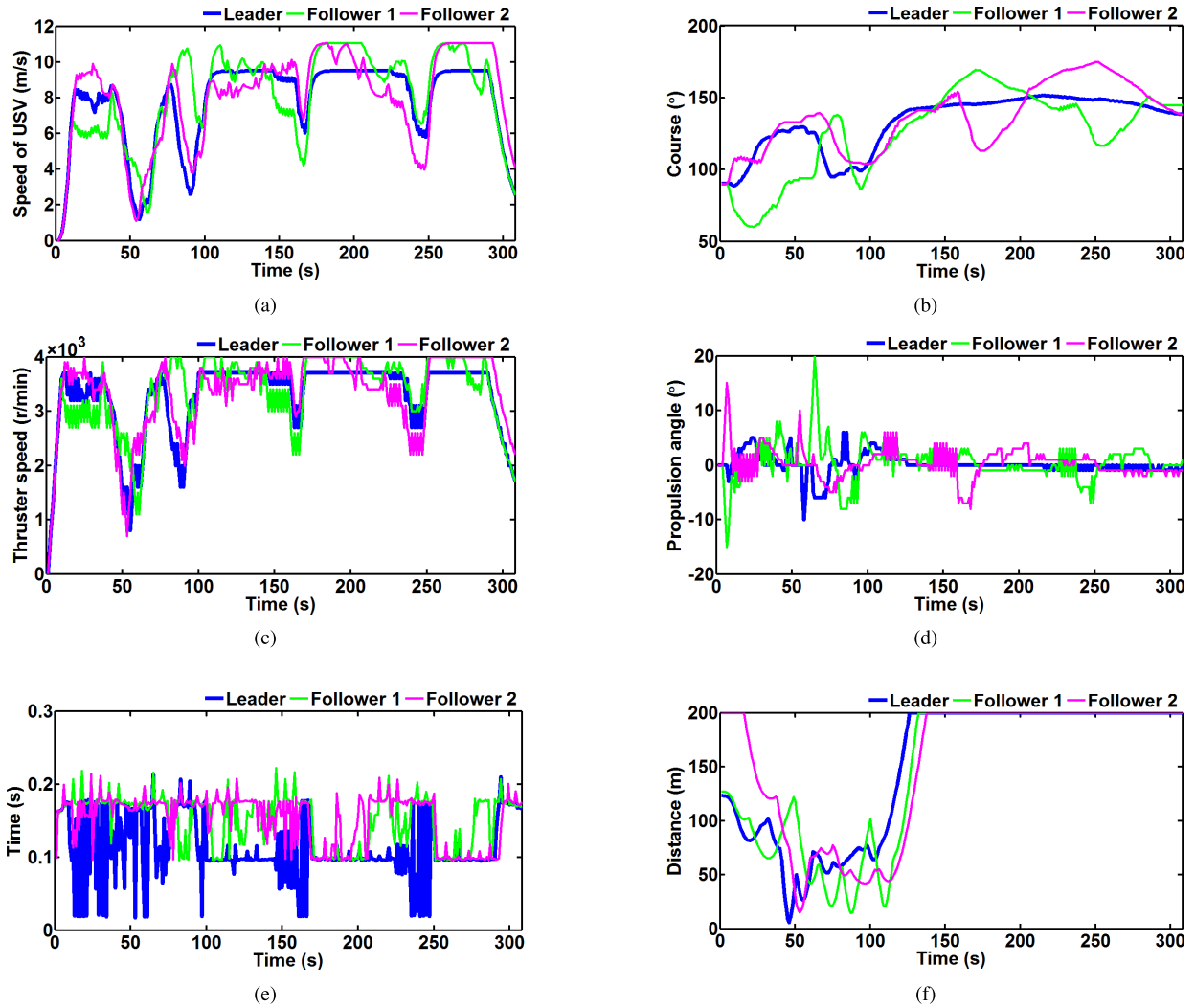

FIGURE 9. Evaluation results of Test two. (a) Speed V of USV. (b) Course ψ of USV. (c) Thruster speed n. (d) Propulsion angle δ. (e) Computation time T. (f) Distance D between obstacles and USV.

The effectiveness of the FCAS is verified by Matlab simulation on the computer equipped with 4 GB of RAM and a Core i7 3.6 GHz processor. The simulation results show in the motion sequence diagram. In the diagram, the colors associated with Leader, Follower 1 and Follower 2 are blue, red and magenta. The '+' and '*' are markers for start and end points, and the end point is extended to a red circular area. The green curves is the current predicted trajectories of USV. For dynamic obstacles (DOs), the positions of DO1, DO2 and DO3 are represented by cyan, yellow and green circles, and when they enter the detection area, the color turns magenta.

A. TEST ONE

In the test, the dimensions of simulation area are 2400 m × 2200 m, and 30 static circular obstacles with radius between 10 m and 60 m are randomly generated in the area [0–1000, 0–1000] m.

Figure 6 is a motion sequence diagram of USV formation in Test one. To verify the formation forming ability, the positions of the Followers are reversed at the beginning in Figure 6(a). Figure 6(b) describes the formation forming process. Figure 6(c) shows the scene of USV formation sailing in restricted waters. After passing through restricted water, formation enters open water, as shown in Figure 6(d). Figure 6(e) shows that USVs stability maintain desired formation shape. Figure 6(f) describes that the USVs arrive at their respective ending area.

Figure 7 compares the main parameters of the three USVs, and Table 2 is their evaluation index. Figures 7(a-d) show the control input (n, δ) and state output (V, ψ) of the USVs throughout the process. The USVs maintain maximum speed as far as possible and adjust speed according to risk level and formation constraint condition. In Figure 7(d), the propulsion angle values of Followers are larger at the beginning, which is due to form formation. After that, the propulsion angle is less than 10°, so the system is stable. Figure 7(e) is the computing time T for each FCAS in the formation, and the maximum computing time of 0.21 s is much less than the

control update interval $\Delta t_c = 1.0$ s. Figure 7(f) describes the distance D between each USVs and the detected obstacles in the distance range d_r, and their minimum distance is 16.4 m with average distance 147.9 m. So the USV formation safely avoids all obstacles to the end. In Figure 7(g), from 230 s to 260 s, in open waters, the formation remains stable and follows the Leader to the end, while the formation keeping error E is less than 10 m. In this period, the minimum keeping error is 1.3 m and 2.3 m, thus the stable formation keeping for USVs is achieved.

B. TEST TWO

The three performance of the system is preliminarily verified by static environment simulation in Test one. To better verify the applicability in restricted water, on the basis of Test one, three dynamic obstacles (DO1, DO2 and DO3) with the radius of 20 m and speed of 10 m/s, 10 m/s, and 7 m/s are added. For the formation forming ability, at 120 s and 200 s, the system begins to perform two formation transformation tasks respectively by exchanging the Follower's sub-targets.

In Figure 8, the cyan circles with number 1, 2 and 3 are the DO1, DO2 and DO3. When the time is 49 s, DO1 and Follower 2 are in a crossing situation, which forces the Follower 2 to decelerate. Next, Leader completely avoids DO2, and Follower 1 are avoiding DO1 at 59 s. After 85 s, the formation completely avoids the DO1 and DO2, and began to evade the DO3. At 162 s, the formation is executing the first formation transformation task. After completing the first task, the vessels continue to perform second formation transformation task, as shown in Figure 8(e). Finally, at 308 s, the formation completes these tasks and reaches the ending area.

TABLE 3. Results of evaluation index about USVs in test two.

USV	Index	V(m/s)	n(r/min)	δ(°)	T(s)	D(m)
Leader	maximum	9.5	3700	6.0	0.21	200.0
	minimum	0.0	0	-10.0	0.02	5.7
	average	7.7	3263	0.1	0.11	150.9
Follower 1	maximum	11.1	4000	20.0	0.22	200.0
	minimum	0.0	0	-15.0	0.10	14.8
	average	8.1	3344	0.4	0.15	147.1
Follower 2	maximum	11.1	4000	15.0	0.21	200.0
	minimum	0.0	0	-8.0	0.10	15.2
	average	8.0	3341	0.4	0.15	153.4

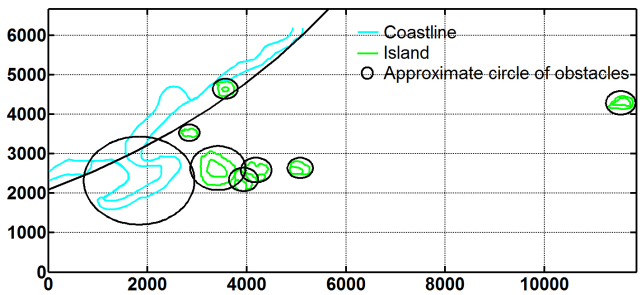

FIGURE 10. The actual sea environment model.

Compared with Test one, the evaluation index is almost the same except for D and δ in Table 3. In Figure 9(a-d), the formation avoids dynamic obstacles and completes the formation transformation tasks by adjusting the δ, and maintains the rapidity as far as possible. Figure 9(e) is the computing time of each FCAS with the maximum computing time of 0.22 s. For the distance D, because the Test two is more complex than Test one, their minimum distance becomes smaller, but the formation still safely passes through the complex scenario and completes the formation transformation tasks.

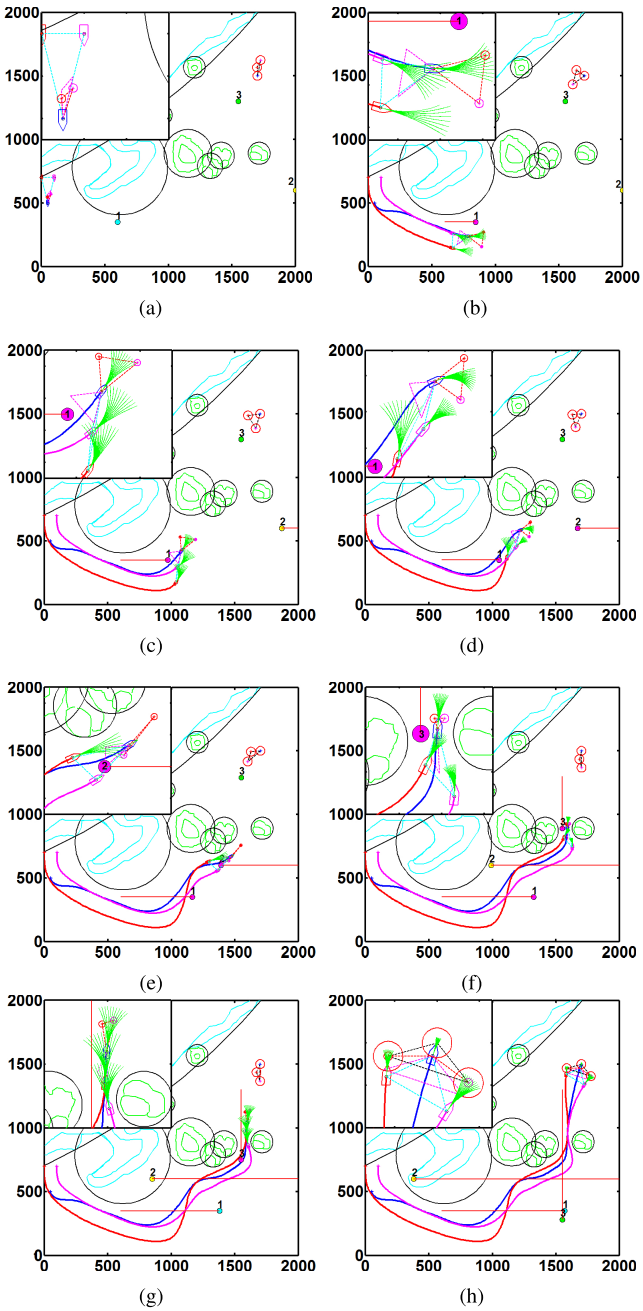

FIGURE 11. The motion sequence diagram of Test three. (a) Time 1 s. (b) Time 80 s. (c) Time 112 s. (d) Time 132 s. (e) Time 160 s. (f) Time 200 s. (g) Time 214 s. (h) Time 261 s.

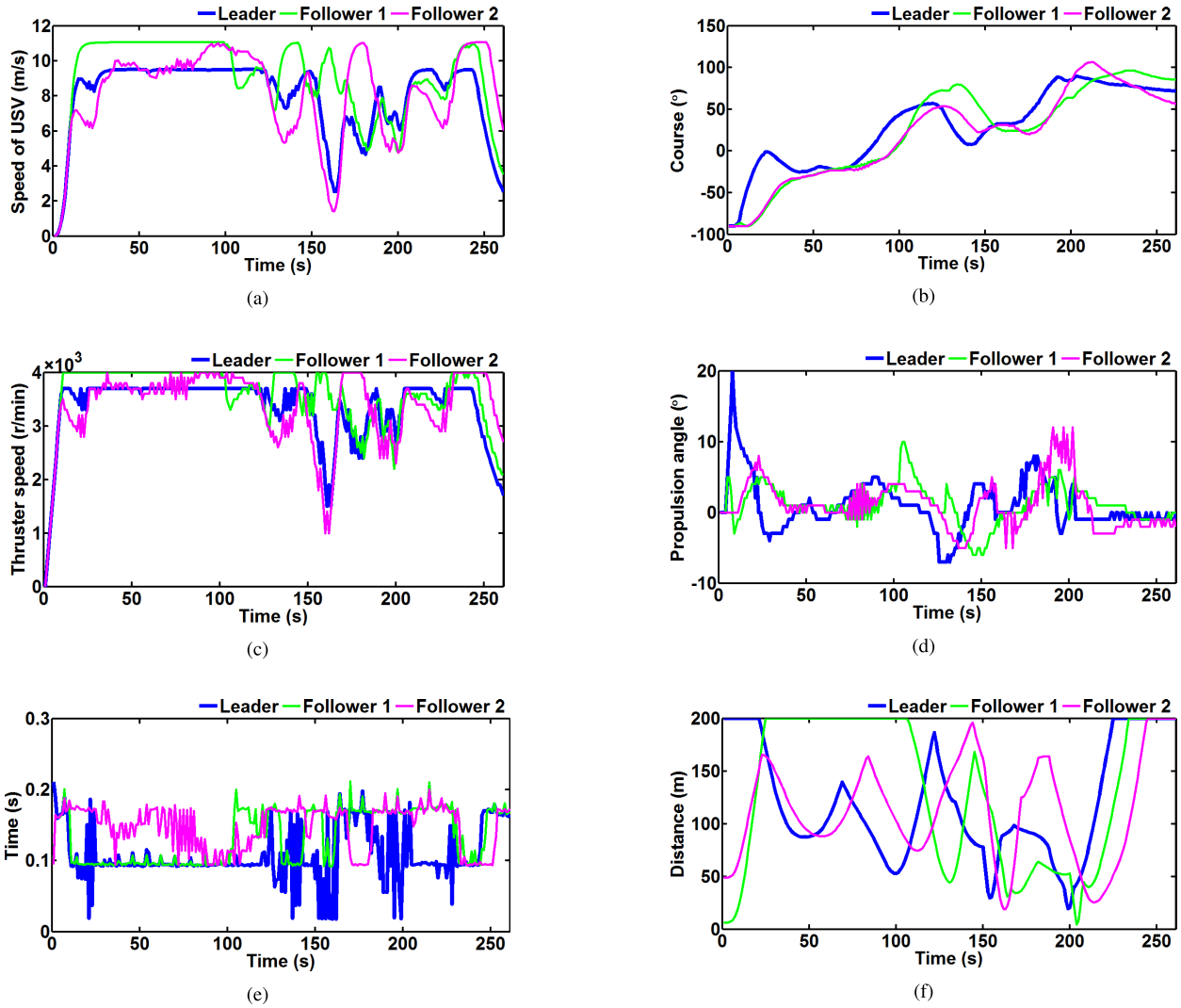

FIGURE 12. Evaluation results of Test three. (a) Speed V of USV. (b) Course ψ of USV. (c) Thruster speed n. (d) Propulsion angle δ. (e) Computation time T. (f) Distance D between obstacles and USV.

C. TEST THREE

The outer sea area of the harbor basin at Dalian Maritime University marine is selected as the environment modeling area, which is built by expanding the island and coastline into the circle [31], as shown in Figure 10.

Because the open water cannot effectively test the algorithm, the map has been reduced by 3 times to make the environment more complex. The system parameters are still consistent with the first two tests, and three DOs and a formation transformation task are added into the test, where the speed of DOs are 4 m/s, 10 m/s and 10 m/s. The movement sequences are represented in Figure 11. Figure 11(a), 11(b) depict the trajectory of the formation leaving its initial position and meeting the DO1 to form a overtaking situation, in which case the FCAS control formation to change course without slowing down. At 30 s, the formation transformation task is executed, and then through the transition, the desired shape of formation are completed at 80 s. Figure 11(b-d) show the process of forming a new formation shape while avoiding DO1. Then, from 160 s - 200 s, the formation continuously evades DO2 and DO3. The formation is in restricted water when the DO3 is avoided, and at 261 s, the formation reaches safely the ending area.

The results of USVs input and output with realistic sea environment are shown in Figures 12(a-d) and Table 4. In Figure 12(a), 12(c), as the Follower 1 is far away from

TABLE 4. Results of evaluation index about USVs in test three.

USV	Index	V(m/s)	n(r/min)	δ(°)	T(s)	D(m)
Leader	maximum	9.5	3700	20.0	0.21	200.0
	minimum	0.0	0	-7.0	0.02	19.5
	average	8.0	3344	1.0	0.11	120.3
Follower 1	maximum	11.1	4000	10.0	0.21	200.0
	minimum	0.0	0	-6.0	0.09	4.3
	average	9.0	3564	1.2	0.13	130.9
Follower 2	maximum	11.1	4000	12.0	0.20	200.0
	minimum	0.0	0	-5.0	0.09	19.0
	average	8.2	3371	1.1	0.15	113.5

the obstacles on the outside of the formation, it needs to take more distance, so the speeds of Follower 1 and it's thruster quickly increases to the highest speed and maintains the speed at the beginning. When the thruster speed of the Follower is lower than Leader by n_c, the Leader will slow down appropriately to ensure formation maintenance in Figure 12(c). From Figure 12(d), during the whole test process, except that the leader's propulsion angle reaches the climax value of 20° to adjust the course at the beginning, their propulsion angles are always less than 12° after that. The computing time is basically the same as the first two tests in Figure 12(e). In Figure 12(f), their minimum distances are 19.5 m, 4.3 m, and 19.0 m, which means that the formation is safe.

VI. CONCLUSION

This paper considers the autonomous navigation of USV formation in complex environments and presents a novel formation collision avoidance system (FCAS) for improving the autonomy of USVs in the present of multi-obstacles. The FCAS is developed based on the FCS-MPC principle, which not only combines path planner with controller, but also reduces computational load. Furthermore, the thruster speed and propulsion angle instead of force and torque are the control outputs of the FCAS, which is more practical. By adopting the leader-follower structure, multiple vessels can be used to achieve the USV clusters. And the distributed control strategy can solve the problem of internal collision avoidance within the formation. Besides, the experiments are implemented under the simulated marine environments and the results have illustrated the formation stability, formation forming ability and the applicability in restricted water of the proposed FCAS. The formation scheme can also be extended to the other marine formation system.

In terms of the future work, the FCAS proposed will be improved in several ways. First, the environment model can be more practical. Second, because the actual marine environment is complex and changeable, external disturbances need to be considered. Thirdly, the USV formation also should comply with the Convention on the International Regulations for Preventing Collisions at Sea (COLREGs).

REFERENCES

[1] S. Campbell, W. Naeem, and G. W. Irwin, "A review on improving the autonomy of unmanned surface vehicles through intelligent collision avoidance manoeuvres," *Annu. Rev. Control*, vol. 36, no. 2, pp. 267–283, 2012.

[2] Z. Liu, Y. Zhang, X. Yu, and C. Yuan, "Unmanned surface vehicles: An overview of developments and challenges," *Annu. Rev. Control*, vol. 41, pp. 71–93, Jan. 2016.

[3] S.-L. Dai, S. He, H. Lin, and C. Wang, "Platoon formation control with prescribed performance guarantees for USVs," *IEEE Trans. Ind. Electron.*, vol. 65, no. 5, pp. 4237–4246, May 2018.

[4] L. Liu, D. Wang, Z. Peng, and H. H. T. Liu, "Saturated coordinated control of multiple underactuated unmanned surface vehicles over a closed curve," *Sci. China Inf. Sci.*, vol. 60, no. 7, 2017, Art. no. 070203.

[5] Z. Sun, G. Zhang, Y. Lu, and W. Zhang, "Leader-follower formation control of underactuated surface vehicles based on sliding mode control and parameter estimation," *ISA Trans.*, vol. 72, pp. 15–24, Jan. 2018.

[6] W. Xie, B. Ma, T. Fernando, and H. H.-C. Iu, "A new formation control of multiple underactuated surface vessels," *Int. J. Control*, vol. 91, no. 5, pp. 1011–1022, 2018.

[7] J. Ghommam and M. Saad, "Adaptive leader–follower formation control of underactuated surface vessels under asymmetric range and bearing constraints," *IEEE Trans. Veh. Technol.*, vol. 67, no. 2, pp. 852–865, Feb. 2018.

[8] Y.-Y. Chen and Y.-P. Tian, "Formation tracking and attitude synchronization control of underactuated ships along closed orbits," *Int. J. Robust Nonlinear Control*, vol. 25, no. 16, pp. 3023–3044, 2015.

[9] B. Xiao, X. B. Yang, and X. Huo, "A novel disturbance estimation scheme for formation control of ocean surface vessels," *IEEE Trans. Ind. Electron.*, vol. 64, no. 6, pp. 4994–5003, Jun. 2017.

[10] X. Jin, "Fault tolerant finite-time leader–follower formation control for autonomous surface vessels with LOS range and angle constraints," *Automatica*, vol. 68, pp. 228–236, Jun. 2016.

[11] Z. Gao and G. Guo, "Fixed-time leader-follower formation control of autonomous underwater vehicles with event-triggered intermittent communications," *IEEE Access*, vol. 6, pp. 27902–27911, 2018.

[12] Z.-Q. Liu, Y.-L. Wang, and T.-B. Wang, "Incremental predictive control-based output consensus of networked unmanned surface vehicle formation systems," *Inf. Sci.*, vols. 457–458, pp. 166–181, Aug. 2018.

[13] H. Rezaee and F. Abdollahi, "A decentralized cooperative control scheme with obstacle avoidance for a team of mobile robots," *IEEE Trans. Ind. Electron.*, vol. 61, no. 1, pp. 347–354, Jan. 2014.

[14] D. Xu, X. Zhang, Z. Zhu, C. Chen, and P. Yang, "Behavior-based formation control of swarm robots," *Math. Problems Eng.*, vol. 2014, no. 1, 2014, Art. no. 205759.

[15] A. Askari, M. Mortazavi, and H. A. Talebi, "UAV formation control via the virtual structure approach," *J. Aerosp. Eng.*, vol. 28, no. 1, 2015, Art. no. 04014047.

[16] Y. Hao and S. K. Agrawal, "Planning and control of UGV formations in a dynamic environment: A practical framework with experiments," *Robot. Auton. Syst.*, vol. 51, nos. 2–3, pp. 101–110, 2005.

[17] M. Saska, V. Spurný, and V. Vonásek, "Predictive control and stabilization of nonholonomic formations with integrated spline-path planning," *Robot. Auto. Syst.*, vol. 75, pp. 379–397, Jan. 016.

[18] Y. Liu and R. Bucknall, "The angle guidance path planning algorithms for unmanned surface vehicle formations by using the fast marching method," *Appl. Ocean Res.*, vol. 59, pp. 327–344, Sep. 2016.

[19] P. Urcola, M. T. Lázaro, J. A. Castellanos, and L. Montano, "Cooperative minimum expected length planning for robot formations in stochastic maps," *Robot. Auton. Syst.*, vol. 87, pp. 38–50, Jan. 2017.

[20] T. Lee, H. Kim, H. Chung, Y. Bang, and H. Myung, "Energy efficient path planning for a marine surface vehicle considering heading angle," *Ocean Eng.*, vol. 107, pp. 118–131, Oct. 2015.

[21] H. Xiao, Z. Li, and C. L. P. Chen, "Formation control of leader–follower mobile robots' systems using model predictive control based on neural-dynamic optimization," *IEEE Trans. Ind. Electron.*, vol. 63, no. 9, pp. 5752–5762, Sep. 2016.

[22] W. Zhao and T. H. Go, "Quadcopter formation flight control combining MPC and robust feedback linearization," *J. Franklin Inst.*, vol. 351, no. 3, pp. 1335–1355, 2014.

[23] J. Liu, P. Jayakumar, J. L. Stein, and T. Ersal, "Combined speed and steering control in high-speed autonomous ground vehicles for obstacle avoidance using model predictive control," *IEEE Trans. Veh. Technol.*, vol. 66, no. 10, pp. 8746–8763, Oct. 2017.

[24] C. Xia, T. Liu, T. Shi, and Z. Song, "A simplified finite-control-set model-predictive control for power converters," *IEEE Trans. Ind. Informat.*, vol. 10, no. 2, pp. 991–1002, May 2014.

[25] T. I. Fossen, *Marine Control Systems Guidance, Navigation, and Control of Ships, Rigs and Underwater Vehicles*. Trondheim, Norway: Marine Cybernetics, 2002.

[26] D. Mu, G. Wang, Y. Fan, X. Sun, and B. Qiu, "Adaptive LOS path following for a podded propulsion unmanned surface vehicle with uncertainty of model and actuator saturation," *Appl. Sci.*, vol. 7, no. 12, p. 1232, 2017.

[27] X.-L. Jia and Y.-S. Yang, *The Mathematical Model of Ship Motion Mechanism Modeling and Identification Modeling*. Dalian, China: Dalian Maritime University Press, 1999.

[28] X.-J. Sun, L.-L. Shi, Y.-S. Fan, and G.-F. Wang, "Online parameter identiflcation of usv motion model," *Navigat. China*, vol. 1, no. 1, pp. 39–43, 2016.

[29] D. Mu, G. Wang, Y. Fan, X. Sun, and B. Qiu, "Modeling and identification for vector propulsion of an unmanned surface vehicle: Three degrees of freedom model and response model," *Sensors*, vol. 18, no. 6, p. 1889, 2018.

[30] X. Sun, G. Wang, Y. Fan, D. Mu, and B. Qiu, "Collision avoidance using finite control set model predictive control for unmanned surface vehicle," *Appl. Sci.-Basel*, vol. 8, no. 6, p. 926, Jun. 2018.
[31] N. Wang, X. Meng, Q. Xu, and Z. Wang, "A unified analytical framework for ship domains," *J. Navigat.*, vol. 62, no. 4, pp. 643–655, 2009.

XIAOJIE SUN received the M.E. degree in control engineering from Dalian Maritime University, Dalian, China, in 2016, where he is currently pursuing the Ph.D. degree in control theory and control engineering. His research interests include sea traffic management and unmanned surface vehicle systems, such as formation and collision avoidance.

GUOFENG WANG received the B.E., M.E., and Ph.D. degrees from Dalian Maritime University, Dalian, China, where he is currently a Professor with the College of Marine Electrical Engineering. He is involved in the technical research of the marine automation system and automation equipment, and has presided over and participated in a number of national and ministerial projects. His research interests include ship automation, advanced ship borne detection device, and advanced power transmission.

YUNSHENG FAN received the B.E., M.E., and Ph.D. degrees from Dalian Maritime University, Dalian, China, in 2004, 2007, and 2012, respectively, where he is currently an Associate Professor with the College of Marine Electrical Engineering. His research interest includes ship intelligent control and its application.

DONGDONG MU received the M.E. degree in control theory and engineering from Dalian Maritime University, Dalian, China, in 2015, where he is currently pursuing the Ph.D. degree in control theory and control engineering. His research interests include modeling and intelligent control of unmanned surface vehicle.

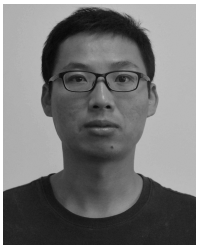

BINGBING QIU received the M.E. degree in control theory and engineering from Dalian Maritime University, Dalian, China, in 2017, where he is currently pursuing the Ph.D. degree in control theory and control engineering. His research interests include nonlinear control and intelligent control of unmanned surface vehicle.